

Current-Pumped Abrupt-Junction Varactor Power-Frequency Converters

BARRY S. PERLMAN, MEMBER, IEEE

Abstract—This paper presents equations and design curves for a noninverting frequency converter which will enable the engineer to design efficient, high-level parametric devices using abrupt-junction varactors. In addition, the excellent intermodulation characteristic and extremely wide dynamic range (in excess of 140 dB) of the parametric frequency converters enables their use immediately as low-frequency downconverters or microwave upconverters without any deterioration of other parameters, such as noise figure, in system performance. It has been shown that these abrupt-junction diode devices possess the largest known dynamic range, in addition to being relatively spurious free with respect to intermodulation products produced by the diode nonlinearity, intermodulation distortion being generated in the device due only to gain saturation.

The design curves also indicate the maximum conversion efficiency possible with a given abrupt-junction diode. An inflection point for 50 per cent conversion efficiency occurs for all diodes. Any additional improvement in pump-to-sideband efficiency greater than 50 per cent gained by adjusting the diode and circuit performance, requires relatively large increases in the diode cutoff frequency and reduction in overall circuit losses. Other design curves include impedance variation with drive powers and the overall limiting output power capability for a given diode. A design example is presented to demonstrate the usefulness of the derived results and design curves. The experimental results obtained with this design have demonstrated a microwave, C band, tunable converter with almost 50 per cent conversion efficiency.

I. INTRODUCTION

THE VARACTOR diode has become well known as an excellent device for low-noise amplification [1], [2], [3]. Recently, however, the varactor diode has been used in high-level frequency converters as both a means of obtaining large amounts of power tunable over wide bandwidths and as a means of placing FM and PM information on a CW source such as a varactor multiplier. The high-level parametric upconverter differs from a low-noise parametric amplifier in the area of conversion efficiency.

Several papers have been published which present a general discussion of the properties of large signal varactor parametric devices [1]–[5]. In each case, only approximate solutions for the transfer impedances¹ are derived. It is usually shown that these impedances are affected by the powers present in all circuits and, therefore,

Manuscript received June 9, 1964; revised October 5, 1964. The work disclosed in this paper was partially sponsored by Signal Corps Contract DA-36-039-AMC-02345(E), "Interference Reduction Techniques."

The author is with the Communication Systems Div., RCA, New York, N. Y.

¹ These impedances are defined as the "effective" real input impedance looking into the device at a specific port (one frequency), excluding all circuit losses, when the diode is conducting currents at all the required frequencies.

fore, are the basis of the onset of saturation in any parametric device.

One of the problems in the large-signal solution for a varactor-frequency converter is the infinite number of terms found when attempting to evaluate the Taylor expansion for charge as a function of voltage for an arbitrary varactor. If one reverses this approach and finds the expansion for voltage as a function of charge, with a junction exponent² γ of $\frac{1}{2}$, it is found that the series is finite and easily utilized to find a more exact solution for the diode transfer impedance. A study of the interrelationship between these respective circuit impedances, with regard to the conversion efficiency between the desired frequencies, yields an optimum design procedure.

A diode which exhibits a capacitive junction exponent² γ of $\frac{1}{2}$ is known as an "abrupt" junction varactor. The junction exponent is a function of the dopant concentration as a function of distance from the junction. Normally, diodes exhibit γ 's between $\frac{1}{3}$ to $\frac{1}{2}$, the $\frac{1}{3}$ exponent signifying a "graded" junction. If the exponent γ is greater than $\frac{1}{2}$, the device is referred to as hyperabrupt and is characterized by high-conversion efficiency for high-harmonic orders [6]. When diodes are used which yield an abrupt capacitance variation over their entire voltage swing 0– V_B breakdown, this analysis would yield exact results if it were not for a limited allowed forward conduction. For all intents and purposes, it will be shown that the "normal" available varactors, where $\gamma \approx 0.45$, yield results approaching those achievable as indicated by this analysis. Although mathematically convenient, this analysis for the abrupt-junction device is also based upon consideration of the higher achievable conversion efficiencies and power levels attainable when using this device as compared to the common, graded junction diode. It will be shown that the allowable drive powers may be significantly higher for an abrupt diode due to a greater maximum stored charge. It has been shown [3], [6] that the transfer impedance for an active varactor increases with increasing γ thereby producing higher operating efficiencies when considering the relative level of losses.

Another interesting characteristic of abrupt-junction

² The junction exponent determines the reactance-voltage nonlinearity and is defined in Section II.

devices is that they are relatively spuria free. Since the expansion of voltage produced as a function of charge terminates in the second derivative, the device is truly "square law." Higher-order harmonics are not produced above the second, and third-order intermodulation terms do not appear as a result of the diode nonlinearity. Intermodulation products will be produced, however, due to the gain saturation process that occurs due to large signal operation.

The second primary consideration in this analysis is the fact that we have specified voltage as a function of charge. Since the charge is the independent variable, it becomes necessary to pump the device with current, the time integral of charge. The "current-pumped" mode of operation yields mathematically convenient relations based upon a practically achievable network configuration. Figures 1 and 2 indicate the relative difference between a diode which is made voltage dependent (Fig. 1) and one which is mesh-current dependent (Fig. 2). The tuned networks allow only the representative voltage or current, Figs. 1 and 2, respectively, to be developed in that circuit. It must be pointed out here that a voltage-pumped junction, excluding R_s , is impossible to achieve. The real diode, which consists of a series loss resistance and a nonlinear junction reactance, will conduct many currents, resulting in a nonlinear voltage drop across R_s . The actual resulting voltage across the junction thus becomes nonlinear. By specifying the mesh currents shown in Fig. 2 to be the only allowed currents, the series representation of the varactor may be effectively utilized as the basis of an exact solution for the resulting terminal voltages.

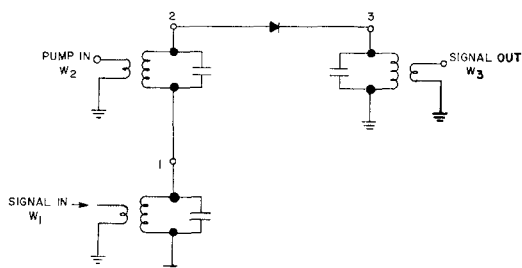


Fig. 1. Voltage-pumped diode converter.

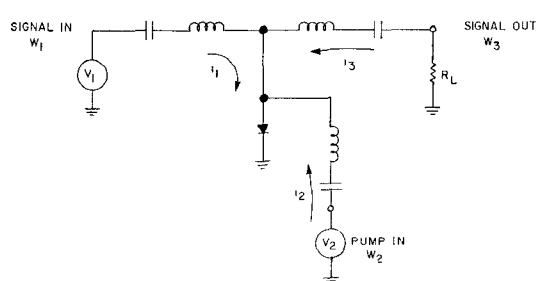


Fig. 2. Current-pumped diode converter.

II. BASIC RELATIONS

A typical varactor diode, reverse biased, is characterized by a junction capacitance which is voltage dependent, as shown in (1).

$$C(V) = \frac{C(0)}{\left[1 + \frac{V}{V_c}\right]^\gamma} = C_{\min} \frac{(V_c + V_B)^\gamma}{(V_c + V)^\gamma} \quad (1)$$

where

$C(0)$ = zero-bias capacitance

C_{\min} = junction capacitance at V_B

V_B = breakdown voltage

V_c = contact potential (~ 0.5 V for abrupt junction)

V = total applied external voltage

γ = junction exponent: $\frac{1}{2}$ —abrupt

$\frac{1}{3}$ —graded

$> \frac{1}{2}$ —hyperabrupt

The inverted representation of $C(V)$ [the elastance function $S(V)$] may be expressed as [1], [3]

$$S = S_m \left(\frac{Q}{Q_m} \right)^{\gamma/(1-\gamma)} \quad (2)$$

where

Q_m = maximum charge (at breakdown V_B)

S_m = maximum elastance ($= 1/C_m$)

From (1), (2), the diode-junction voltage may be written as

$$V + V_c = (V_B + V_c) \left(\frac{Q}{Q_m} \right)^{1/(1-\gamma)} \quad (3)$$

which becomes

$$V + C_c]_{\gamma=1/2} = (V_B + V_c) \left[\frac{Q}{Q_m} \right]^2 = \frac{1}{2} \frac{S_m}{Q_m} Q^2 \quad (4)$$

$$V + V_c]_{\gamma=1/3} = \frac{2}{3} \frac{S_m}{Q_m^{1/2}} Q^{3/2} \quad (5)$$

Figure 3 is a normalized plot of (4) and (5), where the maximum charge has been referred to that of the abrupt junction. Figure 4 using (2), indicates the elastance-linearity condition, with charge as the independent variable, for the abrupt diode.

Examination of these last two equations and Figs. 3 and 4, indicates the true square-law characteristics of the abrupt-junction device, which may be used with a linear-time variation of charge to obtain a linear variation in elastance (current pumping defined), whereas a voltage-pumped diode results in a nonlinear variation of elastance and, thus, is not capable of providing the same high-output efficiencies.³ In addition, in order to

³ This property of the current-pumped abrupt-junction diode is discussed in Rafuse and Penfield [1], ch 7.

effectively voltage pump a diode junction from a sinusoidal source, no series losses are permitted since the current, being nonlinear ($i_d = dq/dt$), would result in a nonlinear drop across R_{losses} and, consequently, a nonlinear voltage across C_{diode} .

As shown by Fig. 3, the graded junction may support only $\frac{3}{4}$ of the abrupt junction's maximum charge; $Q_{m \text{ graded}} = \frac{3}{4} Q_{m \text{ abrupt}}$ for equal S_m and $(V_B + V_c)$.

For abrupt diode:

$$Q_{m_a} = 2 \frac{(V_c + V_B)}{S_m} \quad (6)$$

For graded diode:

$$Q_{m_g} = \frac{3}{2} \frac{V_c + V_B}{S_m} \quad (7)$$

Thus, the power-handling capability of the graded junction may be shown to be less than that of the abrupt if one considers that maximum drive power is proportional to the current squared, the time derivative of the instantaneous diode charge.

To provide full sinusoidal current pumping, which corresponds to a voltage swing across the diode junction between 0 bias and V_B , the bias charge is chosen to be $-Q_m/2$ as shown in Figs. 3 and 4. The corresponding bias voltage then becomes $(V_B + V_c)/4$.

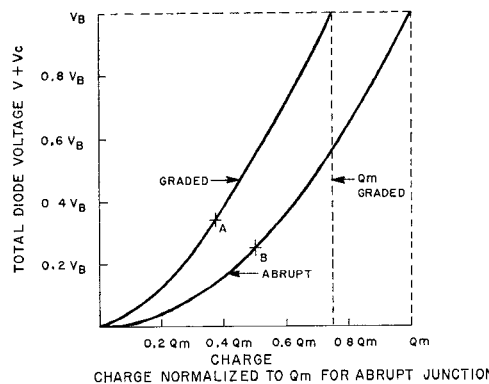


Fig. 3. Voltage as a function of charge.

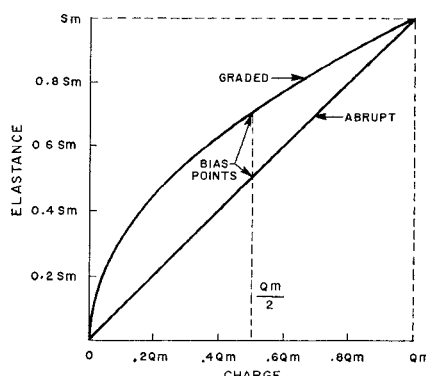


Fig. 4. Elastance-charge curves.

III. UPPER SIDEBAND UPCONVERTER (CURRENT PUMPED)

In the upper sideband mode, the output (at frequency ω_3) is related to the pump (at frequency ω_2) and signal (at frequency ω_1) by

$$\omega_3 = \omega_1 + \omega_2 \quad (8)$$

The respective diode currents may be represented as follows:

$$I_{\text{signal}} = I_1 \cos(\omega_1 t + \theta_1) = i_1 e^{j\omega_1 t} + i_1 * e^{-j\omega_1 t} \quad (9a)$$

$$I_{\text{pump}} = I_2 \cos(\omega_2 t + \theta_2) = i_2 e^{j\omega_2 t} + i_2 * e^{-j\omega_2 t} \quad (9b)$$

$$I_{\text{output}} = I_3 \cos(\omega_3 t + \theta_3) = i_3 e^{j\omega_3 t} + i_3 * e^{-j\omega_3 t} \quad (9c)$$

where the relative phases are included in the complex currents

$$i_k = \frac{I_k}{2} e^{j\theta_k}$$

$$|i_k| = \frac{I_k}{2} \quad (k = 1, 2, 3) \quad (10)$$

All circuits are assumed to be tuned to resonance, the current phases corresponding to that of their respective source voltage generators

$$v_k = \frac{V_k}{2} e^{j\theta_k} \quad (11)$$

A useful representation similar to that introduced by Rafuse and Penfield [1], is the pumping quality factor M which is the ratio of the instantaneous diode charge to the maximum charge Q_m .

$$M_k = \frac{i_k}{\omega_k Q_m} \quad m_k = |M_k| = \frac{|i_k|}{\omega_k Q_m} \quad (12)$$

The individual circuit resistance comprising circuit loss and diode loss is represented by

$$R_k = R_s + R_{\text{circuit loss}}(k) \quad (13)$$

The effective total source and load impedances become

$$R_{T_k} = R_k + R_{g_k} \quad (k = 1, 2)$$

$$R_{T_3} = R_3 + R_L \quad (k = 3) \quad (14)$$

A schematic representation of the three circuits, tuned to resonance, is shown in Fig. 5.

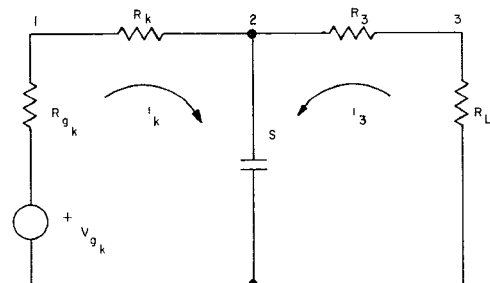


Fig. 5. Input-output circuits

The total charge Q may be represented as the sum of a dc charge ($Q_m/2$) and an ac charge q found by integrating the sum of (9a)–(9c). The input-output network equations are found by substituting the total Q into (4), collecting the terms at equal frequencies, and adding the diode loss $i_k R_s$ and other impedances (i.e., $i_k R_{T_k}$) to the respective equations at their associated frequencies. These results can be expressed in matrix form which may then be used to readily solve for the desirable circuit characteristics (i.e., Z_{in} , Z_{out} , P_{in} , etc.). Table I (next page) indicates the basic device parameters of interest obtained in the latter fashion.

IV. OPTIMUM EFFICIENCY CONDITION

In order to utilize the low-loss conversion properties of this device, the impedance levels⁴ of the device must be made as large as possible with respect to the losses. This results in a minimum value for the ϵ 's⁵ representative of the relative losses. It is to be noted here that an increase in the output-circuit efficiency by increasing the load resistance R_L increases R_{T_3} ($R_{T_3} = R_L + R_3$), thereby reducing the transfer impedances in both the pump and signal circuits [see Table I, a)].

A real impedance match (assuming all reactive circuits tuned to resonance) is established in the signal and pump circuits when,

$$R_{g_2} = R_2 + R_{0_2} = R_2 + \frac{K_2}{R_{T_3}} \quad (15)$$

$$R_{g_1} = R_1 + R_{0_1} = R_1 + \frac{K_1}{R_{T_3}} \quad (16)$$

where,

$$K_2 = \frac{m_1^2 \omega_c^2 R_s^2}{\omega_2 \omega_3} \quad (17)$$

$$K_1 = \frac{m_2^2 \omega_c^2 R_s^2}{\omega_1 \omega_3} \quad (18)$$

using the relation,

$$(\text{Radian-Cutoff frequency}) \omega_c = \frac{S_m}{R_s} \quad (19)$$

⁴ These impedances refer to the transfer and load impedances which exclude circuit losses.

⁵ This result is expected from preliminary considerations of a non-linear-reactance device with no losses where Manley Rowe relations predict

$$\frac{P_0}{P_p} \rightarrow \frac{\omega_0}{\omega_p} = 1 + \frac{\omega_s}{\omega_p}$$

for an upper-sideband, noninverted output.

$$\epsilon_1 = \frac{R_1}{R_{0_1}}; \epsilon_2 = \frac{R_2}{R_{0_2}}; \epsilon_3 = \frac{R_3}{R_L}$$

In order to establish an optimum conversion efficiency between input and output, it will be assumed that the dominant loss is R_s so that the total impedances in the individual circuits are almost equal. In those cases where it is desirable to optimize the allowable pump drive power, it will be shown that a sacrifice in signal-circuit efficiency would permit an increase in available output power. The variation in the signal-circuit loss may be represented as an increase of the loss variable R_1 by an arbitrary multiplier constant α . It may be seen from (15) and (16) that α has no effect on R_{0_2} or R_{0_3} , if K_1 is also increased by α . The increase of K_1 to K_1 requires a permissible increase in m_2^2 and therefore, an increase in both P_2 and P_1 (see Table I-f). It will be seen that the use of $\alpha > 1$ will degrade the optimum pump to output conversion efficiency by reducing the allowable value for $m_1^2 \max$ (Section V-C).

The corresponding output impedance for maximum power transferred to R_L becomes,

$$R_L = R_3 + \frac{K_2}{R_{T_3}} = R_3 + \frac{K_1}{R_{T_1}} \quad (20)$$

A simultaneous solution of (20), (15), and (16) yields the following result for the required optimum source and load impedance:

$$\begin{aligned} R_{g_2} &= R_2 \sqrt{X} \\ R_{g_1} &= R_1 \sqrt{X} \\ R_L &= R_3 \sqrt{X} \end{aligned} \quad (21)$$

where,

$$X = 1 + \frac{K_1}{R_1 R_3} = 1 + \frac{K_2}{R_2 R_3} \quad (22)$$

and

$$R_1 = \alpha R_s \quad (22a)$$

$$\frac{K_1}{K_2} = \frac{R_1}{R_2} \quad (23)$$

$$\left(\frac{m_2}{m_1}\right)^2 = \frac{\omega_1}{\omega_2} \frac{R_1}{R_2} \quad (24)$$

The variable α is an arbitrary signal impedance scaling factor.

We may now substitute the optimized impedances into the appropriate expressions in Table I, in order to obtain a representation of the maximum optimum conditions for this device. Table II is a summary of these results.

TABLE I

	From (29)	From (30)
	Signal to sideband ω_1 to ω_3	Pump to sideband ω_2 to ω_3
a) Input impedance (Z)	$Z_1 = R_{T_1} + \frac{m_2^2 S_m^2}{\omega_1 \omega_3 R_{T_3}}$	$Z_2 = R_{T_2} + \frac{m_1^2 S_m^2}{\omega_2 \omega_3 R_{T_3}}$
b) Current gain	$\frac{i_3}{i_1} = \frac{m_2 S_m}{\omega_1 R_{T_3}}$	$\frac{i_3}{i_2} = \frac{m_1 S_m}{\omega_2 R_{T_3}}$
c) Power-conversion efficiency*	$\eta_{0s} = \frac{P_0}{P_s} = \frac{4 \frac{\omega_3}{\omega_1} R_0 R_g R_L}{R_{T_3} [R_{T_1} + R_{0_1}]^2}$	$\eta_{0p} = \frac{P_0}{P_p} = \frac{4 \frac{\omega_3}{\omega_2} R_{0_2} R_{g_2} R_L}{R_{T_3} [R_{T_2} + R_{0_2}]^2}$
d) Active-transfer impedance	$R_{0_1} = \frac{m_2^2 S_m^2}{\omega_1 \omega_3 R_{T_3}}$	$R_{0_2} = \frac{m_1^2 S_m^2}{\omega_2 \omega_3 R_{T_3}}$
e) Theoretical maximum efficiency [7]	$\eta_{0s_m} = \frac{\omega_3}{\omega_2} \left(\frac{1}{1 + \epsilon_1} \right) \left(\frac{1}{1 + \epsilon_3} \right)$	$\eta_{0p_m} = \frac{\omega_3}{\omega_1} \left(\frac{1}{1 + \epsilon_2} \right) \left(\frac{1}{1 + \epsilon_3} \right)$
f) Input power**	$P_1 = 8m_1^2 \left(\frac{\omega_1}{\omega_c} \right)^2 \frac{P_n}{R_s} [R_1 + R_{0_1}]$	$P_2 = 8m_2^2 \left(\frac{\omega_2}{\omega_c} \right)^2 \frac{P_n}{R_s} [R_2 + R_{0_2}]$

* P_0 = power dissipated at frequency ω_3 in R_L P_s = available signal input power at frequency ω_1 P_p = available pump power at frequency ω_2

** The input power is derived from the relation,

$$P_{in} = 2 |i_{in}|^2 R_{in}$$

and refers to the signal and pump circuits P_1 and P_2 , respectively. The familiar notations, P_N (normalized power) = V_B^2/R_s and ω_c (diode cutoff frequency) = S_m/R_s have been used.

TABLE II
IMPEDANCE OPTIMIZED CONDITION

	Referred to signal	Referred to pump
a) Output efficiency	$\eta_{0s} = \frac{\omega_3}{\omega_1} \frac{\sqrt{X} - 1}{\sqrt{X} + 1}$	$\eta_{0p} = \frac{\omega_1}{\omega_2} \eta_{0s}$
b) Total-device efficiency		$\eta_{0T} = \frac{\eta_{0p}}{1 + \omega_1/\omega_2}$
$\frac{P_0}{P_p + P_s}$		
c) Input power	$P_{1m} = P_s = 8m_1^2 \left(\frac{\omega_1}{\omega_c} \right)^2 P_N \frac{R_1}{R_s} \sqrt{X}$	$P_{2m} = P_p = 8m_2^2 \left(\frac{\omega_2}{\omega_c} \right)^2 P_N \frac{R_2}{R_s} \sqrt{X}$
d) Input impedance	$R_{g_1} = R_1 \sqrt{X}$	$R_{g_2} = R_2 \sqrt{X}$
e) Output impedance		$R_L = R_3 \sqrt{X}$

V. NORMALIZED DESIGN CURVES

Examination of Table II indicates that the quantities shown may be normalized so as to enable universal curves to be plotted.

A. Normalized Impedance Variation

From Table II, d), e), we may represent all the match impedances by a normalized variable R_n where,

$$R_n = \frac{R_{g_1}}{R_1} = \frac{R_{g_2}}{R_2} = \frac{R_L}{R_3} = \sqrt{X} \quad (25)$$

This quantity (61) is plotted in Fig. 6 (page 156).

The value of X corresponding to a particular operating efficiency is computed using the necessary diode and circuit-loss data available. The magnitude of the operating pump level m_1 may be determined from the efficiency-operating point, Fig. 8. A nominal value of 0.20 may be assumed. The actual circuit-load resistance may be slightly lower in value than the calculated value due to the effect of the shunting capacitive reactance at the diode. If this reactance should become appreciable with respect to the nominal value of the junction capacitance, the theoretical conversion efficiency will be reduced. This effect is present in both the pump and output circuits when current pumping is used.

B. Variation in Pump-to-Output Conversion Efficiency η_{op}

We may normalize the output efficiency η_{op} with respect to the frequency ratio as follows:

$$\eta_{opn} = \frac{\omega_2}{\omega_3} \eta_{op} = \frac{(m_1 r)^2}{[1 + \sqrt{1 + (m_1 r)^2}]^2} \quad (26)$$

where (25), and Table II, a) have been used.

Figure 7 is a plot of (26) vs. $K_2/R_2 R_3$.

Figure 8 is a plot of (26) vs. m_1 , with r as a parameter, where

$$r = \sqrt{\left(\frac{\omega_c}{\omega_2 \omega_3}\right)^2 \left(\frac{R_s}{R_2 R_3}\right)^2} \quad (27)$$

r represents a quality factor determined from the diode cutoff frequency ω_c and circuit losses.

C. "Worst-Case" Criteria for Maximum Pumping Variable, $m_{1 \max}$

In order to prevent forward conduction or reverse-diode breakdown, the elastance variation is bounded between S_m and 0 (i.e., $0 \leq S(t)/S_m \leq 1$). Using (2)

$$m_1 + m_2 + m_3 \leq 0.25 \quad (28)$$

where the peak values for the m 's are used, irrespective of phase, in order to indicate a worst-case condition. Using (22), (24), (28),

$$m_{1 \max} = \frac{0.25}{1 + \left[1 + \sqrt{\frac{\eta_{opn}}{1 + \omega_1/\omega_2}} \right] \frac{\omega_1 R_1}{\omega_2 R_2}} \quad (29)$$

$m_{1 \max}$ is shown in Fig. 8, superimposed upon the efficiency curves as a function of η_{opn} with ω_1/ω_2 and R_1/R_2 as parameters.

These vertical curves correspond to the maximum value of m_1 which may exist without permitting the diode voltage to exceed the reverse-breakdown level or permit forward conduction. This limiting value corresponds to the condition where the diode voltage representing each of the three circuits assumes its maximum value simultaneously. If the phase angle between pump and signal voltage sources were chosen to correspond to the value where m_1 assumes their absolute maximum, a slight increase in allowable m_1 would be possible. Since this phase angle is arbitrary, only the worst case will be considered, corresponding to these curves.

The permissible operating region represented by these curves is the area to the left of a given vertical curve. The maximum-conversion efficiency is obtained by the intersection of the r curves with the proper $m_{1 \max}$ characteristic, knowing the circuit losses, frequency ratios, and diode characteristics. If an increase in signal-circuit loss is required (22a), its effect upon $m_{1 \max}$ (29) must be considered with the respect to the achievable efficiency.

D. Maximum Input Power

The normalized input powers become,

$$P_{2mN} = \frac{P_{2m}}{P_N} \frac{\omega_3}{\omega_1} = 8m_1^4 \frac{R_1 R_s}{R_2 R_3} \left(\frac{\sqrt{X}}{X - 1} \right) \quad (30)$$

$$P_{1mN} = \frac{\omega_1}{\omega_2} P_{2mN} \quad (31)$$

where

$$R_1 = \alpha R_s$$

using Table II, c) and (22) substituting for ω_c .

Assuming the diode loss resistance R_s constitutes the total net circuit losses (i.e. $\alpha = 1$),

$$P_{2mN} = 8m_1^4 \sqrt{\frac{1 + \frac{K_2}{R_2 R_3}}{\left(\frac{K_2}{R_2 R_3}\right)}} \quad (32)$$

Figure 9 shows the relationship between the input-pump power and the normalized variable

$$\frac{K_2}{R_2 R_3} = \frac{m_1^2 \omega_c^2}{\omega_2 \omega_3}$$

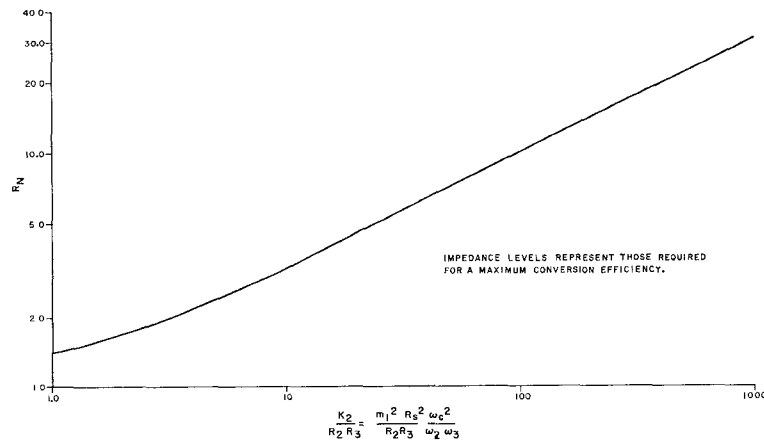
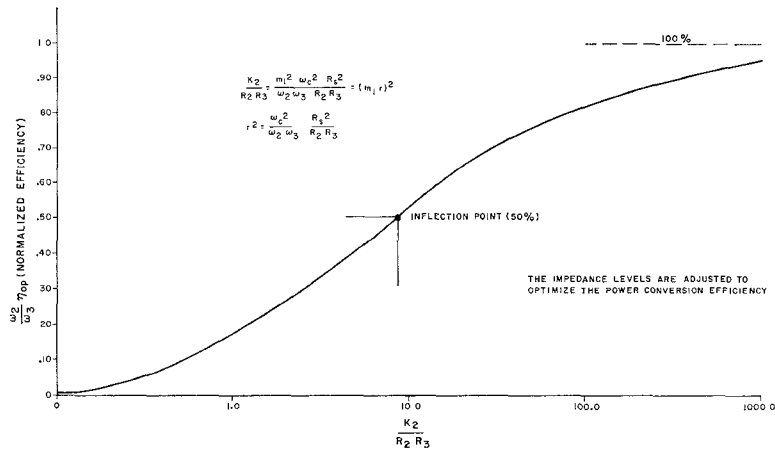
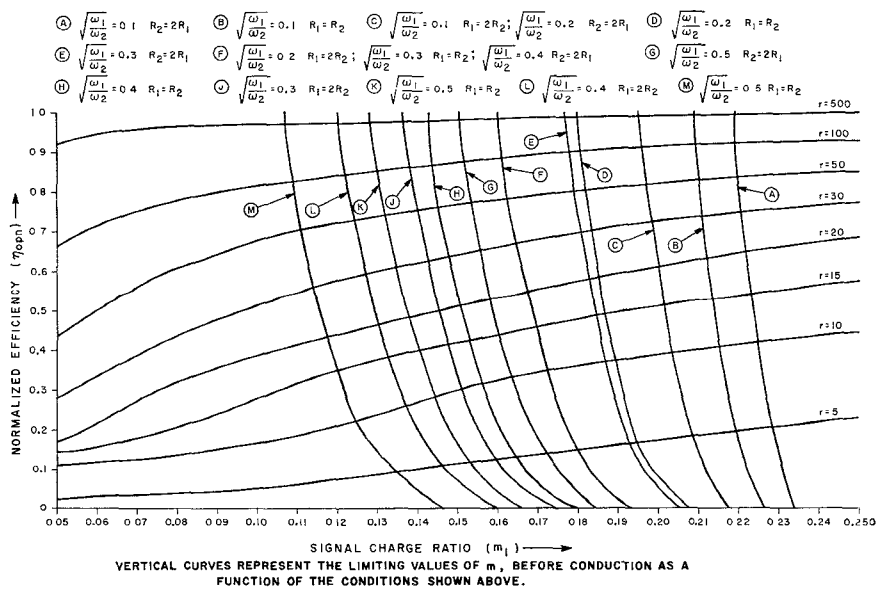
for different values of m_1^2 .

These equations have been derived with the assumption that the effective diode voltage never exceeds a magnitude corresponding to reverse breakdown or forward conduction. In a practical device, the diode is permitted to conduct in the forward direction over a small portion of its normal pump cycle. As a result, a greater power handling capability is obtained in addition to increased operating efficiency. The data represented by the preceding formulas is, therefore, somewhat conservative. The actual operating conditions are expected to exceed the limitations represented here, when an optimum efficiency and power handling capability are to be expected.

E. Output Power

The most important consideration in the design of an efficient power converter is the optimization of the various design parameters with respect to the power (pump)-efficiency product. Although the device is capable of a high-power input at reduced cutoff frequencies, the output power suffers from a very low efficiency of conversion. The reduction in cutoff frequency for a constant pumping parameter m_1^2 corresponds to an increased series resistance R_s and, consequently, a higher dissipation loss.

Taking the product of the two normalized quantities $\eta_{opn} P_{2mN}$ using (26) and (32)

Fig. 6. Normalized impedance variation as a function of quality ratio K_2/R_2R_0 .Fig. 7. Normalized output efficiency η_{0p_n} as a function of the ratio K_2/R_2R_3 .Fig. 8. Normalized output efficiency η_{0p_n} as a function of m_1 .

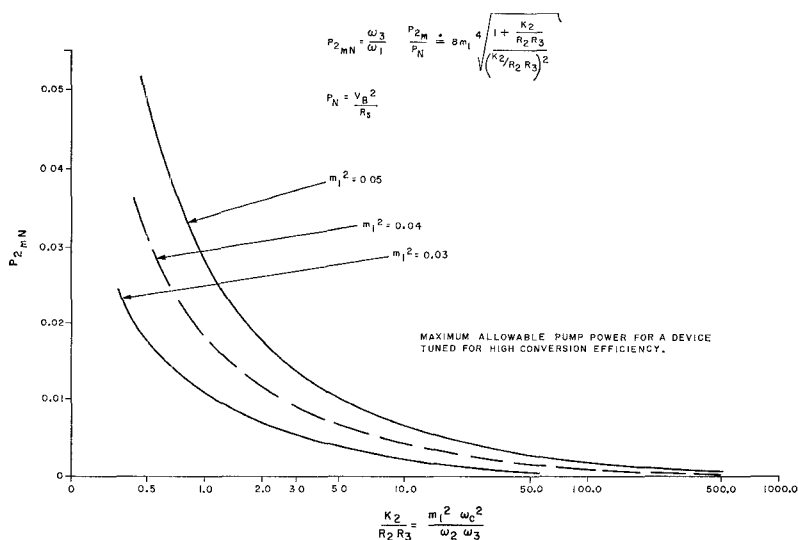


Fig. 9. Normalized input pump power as a function of diode cutoff frequency, operating frequency, and pump ratio m_1 .

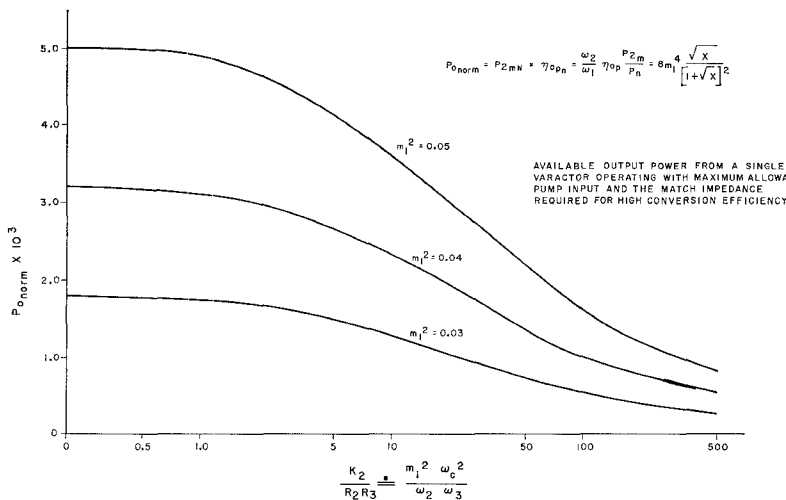


Fig. 10. Normalized output power as a function of conversion efficiency and pump power input.

$$P_{0N} = \eta_{0PN} P_{2mN} = \frac{\omega_2}{\omega_1} \eta_{op} \frac{P_{2m}}{P_N} = 8m_1^4 \frac{\sqrt{X}}{(1 + \sqrt{X})^2} \quad (33)$$

Figure 10 is a plot of this result as a function of

$$\frac{m_1^2 \omega_c^2}{\omega_2 \omega_3} = \frac{K_2}{R_2 R_3}$$

with m_1^4 as a constant parameter. The circuit losses other than R_s have been excluded since both the efficiency and input power are maximized for a minimum loss product $R_2 R_3$. The effect of added circuit losses would be represented on these curves as a reduction in the power $P_{0,norm}$ proportional to the factor $R_1 R_s / R_2 R_3$. If R_1 is increased by α (22a), the pump power may be correspondingly increased, resulting in an increase in available P_0 .

$$P_{0,norm}(\text{Actual}) = \frac{R_1 R_s}{R_2 R_3} P_{0N} \quad (34)$$

The horizontal parameter $K_2 / R_2 R_3$ must be adjusted accordingly.

These curves indicate a slow decrease in output power as a function of the increasing frequency ratio $\omega_c^2 / \omega_2 \omega_3$. The maximum output power is obtained for small values of $K_2 / R_2 R_3$ corresponding to very low conversion efficiencies. In order to attain the high levels of output power specified for $K_2 / R_2 R_3 < 5$, the input pump drive, curve 9, is unnecessarily high. In the neighborhood of $K_2 / R_2 R_3 = 10$ the attainable output power has decreased to 70 per cent of its maximum value. The required pump input has decreased to less than 10 per cent its value at $K_2 / R_2 R_3 = 0.5$, as a result of the increased conversion efficiency. This results in a substantial improvement in operating efficiency with only a minor decrease in output power.

The improvement in efficiency associated with increasing ratio is not significant for $K_2 / R_2 R_3 > 50$ resulting in a limiting output power. The output drops 35 per cent as the parameter $K_2 / R_2 R_3$ is increased from 50 to 500, corresponding to an input change of only 31 per cent. It is thus readily seen that no substantial gain

in conversion efficiency is obtained by increasing the parameter K_2/R_2R_3 beyond approximately 50. The designer may determine the desired operating point depending upon the specific design requirements.

The relative figures used here are for comparison purposes only. An examination of achievable results for a specific low-loss varactor will determine the obtainable results. The data represented by these power curves is a result of a low-loss approximation. The actual circuit data may be readily substituted into the appropriate equations to provide more exact results.

In order to obtain high-efficiency power conversion without sacrificing the power-handling capability of a single diode, multiple diode circuits may be used. Push-pull balanced operation of two or more diodes enables the designer to minimize the number of necessary filters because of the design symmetry. The problem of large signal detuning is also minimized.⁶ Usually the pump and idler sideband filters are not required since push-pull circuits result in a "balanced" cancellation of the output signal in the input-pump port and vice versa. The reduction in the number of filters used results in reduced circuit losses with an increase in the conversion efficiency. The use of several varactors enables one to apply nP_{in} (input power) where n represents the number of varactors. In addition, the overall dynamic range is extended since each individual varactor operates within its linear range regarding its input-output characteristic. Care must be exercised in the circuit design, in order to prevent a runaway condition resulting from an imbalance in the power applied to the individual diodes. The runaway condition corresponds to the case where the number of diodes "operating" in balance are not sufficient to handle the power present, resulting in a sequence of burnouts, effectively increasing the powers across the remaining diodes. The bias networks may be used so as to place the balanced diodes in series in order to minimize detuning effects.

F. Effective Bias

From the original matrix solution mentioned in Section III, one may express the dc component, using (29), as

$$V_{dc} = \left[0.25 + 2m_1^2 \left(1 + \frac{\omega_1 R_1}{\omega_2 R_2} + \frac{\omega_1 \omega_2}{\omega_3^2} \eta_{op} \frac{R_1}{R_3} \right) \right] V_B \quad (35)$$

As an example, if

$$\omega_1 \ll \omega_2, \omega_3; \quad m_1^2 = 0.2$$

then, $V_{dc} \doteq 0.34 V_B$.

The fixed bias voltage required to maintain symmetrical current pumping about the mean charge $q = -Q_m/2$ is $V_B/4$. The additional dc voltage is produced by the nonlinear mixing of the signal frequencies

⁶ Detuning effects tend to be minimized since the odd-order terms in the charge expansion are out of phase when considering the charge developed across each push-pull diode.

in the varactor. A resistor is usually placed in series with the bias supply and the diode, to compensate for variations in the effective diode bias in the presence of power variations. The voltage drop across this resistor is zero *only* for a no-signal condition. Under full-pump conditions, self bias will usually appear across the finite bias source impedance relative to the low diode internal-forward resistance. The effect of this bias is to add to the fixed bias, making it necessary to reduce the fixed-bias supply voltage in order to maintain the effective fixed bias of V_{dc} .

VI. DESIGN AND EXPERIMENTAL RESULTS

A. A Description of Several Possible Circuit Approaches

Because of the inherent symmetry which exists in a push-pull circuit, a large degree of signal isolation may be obtained. In addition, an increase in allowable input power is permitted, proportional to the number of diodes used. It is shown (Appendix) that this type of circuit provides an output at the upper-sideband frequency which may be isolated from the pump circuit, by diode balance, without the need for lossy filters. Tunability is readily attained using the appropriate impedance-matching networks without the added complications associated with low-loss tunable filters. A low-pass filter is necessary in the signal ω_1 port to prevent the pump ω_2 from dissipating in the signal circuit. Since the power-conversion efficiency is usually specified between the pump and output circuits, it is important to minimize the losses in these circuits.

The design shown here may be implemented in either coax, stripline, waveguide, or in a combination, depending upon the operating frequencies and the desired isolation. A possible scheme using symmetrical inputs in coax is shown in Fig. 11. Both the pump and signal enter the diodes through high- and low-pass filters, respectively, in a normal coaxial TEM propagation mode. The resultant sideband (sum frequency idler) is removed from a resonant matching cavity structure by means of a tunable probe. The impedance matching in the coaxial ports is established by realizing a real-part match, using the appropriate filter impedance transformation, and a resonant condition by locating the stop filter in the proper position. Although reference has been made specifically to coaxial networks, stripline structures may be used to advantage in many cases.

A simplified representation of another circuit using *only* coaxial networks, is shown in Fig. 12. This particular circuit uses what might be referred to as a section of coaxial-coax. The diodes are pumped in series by means of a balanced transmission line, which may be designed using the techniques available for constructing "balun transformers." The signal is introduced through a low-pass filter and drives the diodes in the push-pull, parallel mode. The resultant idler is generated in a TEM mode with the conductors acting as a quarter-wave coaxial tuning assembly. The output may

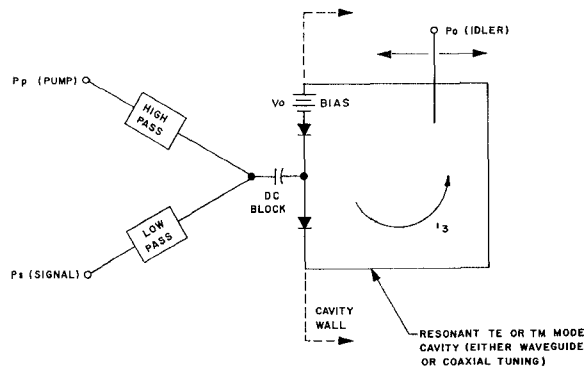


Fig. 11. Coaxial-cavity push-pull converter.

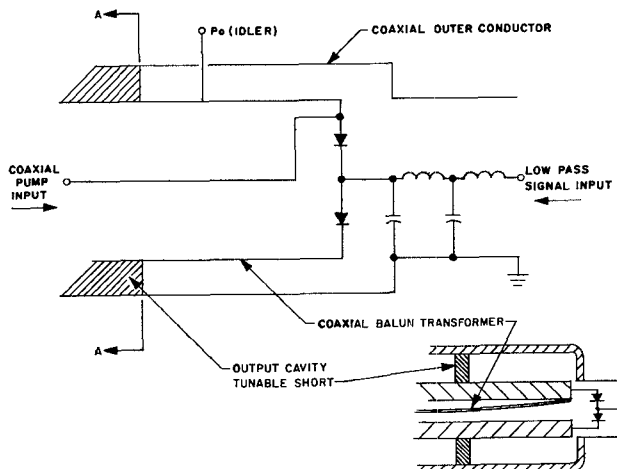


Fig. 12. Coaxial-balun push-pull converter.

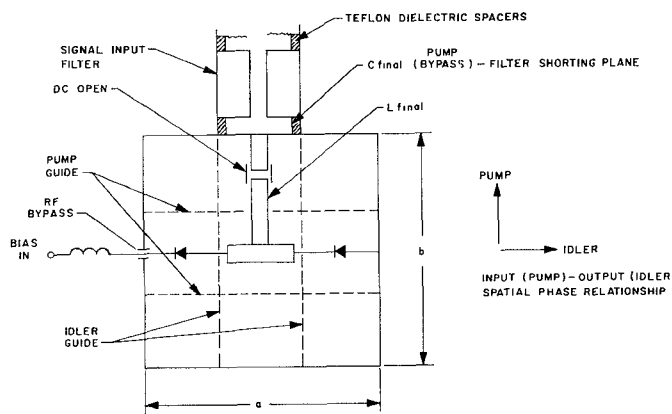


Fig. 13. Waveguide hybrid push-pull converter.

be removed using a current probe coupled to the idler center conductor at the proper impedance tap. The output cavity may be tuned by varying the position of the rear shorting wall (A-A) using sliding finger contacts.

The high-pass pump filter in Fig. 11 may become a section of waveguide. In this case, the pump couples to the diodes by means of an *E*-field probe, the same one used to connect a coaxial low-pass signal circuit to the diode assembly. Figure 13 shows this form of circuit.

The diodes are held in series by a rod which forms a tee structure with the low-pass filter, in a section of nearly square waveguide. Since the pump enters in a TE_{10} mode, in parallel with the varactors, the output (idler) will be effectively rotated into a TE_{01} mode in series with the varactors. This spatial phase relationship between the pump and output accounts for the isolation between these two frequencies. The guide width (*a* dimension with respect to the pump) must be above cutoff for the frequency ω_2 , whereas the *b* dimension may assume a slightly smaller width so as to effect a high-pass filter response for the output. This provides additional isolation between the pump and desired *upper*-sideband output and also rejects the undesired *lower* sideband, which would dissipate power in the output impedance if allowed to circulate.

The necessary impedance matching is established in the waveguide circuits by the use of suitable obstacles. If broadband tuning is desired, a sliding screw tuner may be used to transform the load impedance to the necessary low impedance at the diode plane and also resonate the resultant imaginary component. The low-pass filter may be designed to incorporate the residual elastance of the diodes (Appendix), as well as the inductance associated with the connecting probe. If a Chebyshev, even-order filter prototype is used, the series diode elastance and inductive connecting probe form the filter end section. The final capacitance is located at the upper waveguide shorting plane and acts as the necessary pump-idler bypass and waveguide boundary condition.

B. Design Example

The following example is intended to describe the procedure required to obtain the necessary design details using the previously derived equations. Most currently available diodes do not exhibit an abrupt capacitance variation over the entire voltage swing when reverse biased. It has been found that an average $\gamma = 0.42$ is characteristic of several readily available diodes.

The frequencies of interest in this design are

$$\begin{aligned} \text{Pump} & - f_2 = 4250 \text{ Mc/s} \\ \text{Signal} & - f_1 = 150-750 \text{ Mc/s} \\ \text{Idler} & - f_3 = 4400-5000 \text{ Mc/s} \end{aligned}$$

The diodes chosen for this design have the following specifications:

Dissipation	1 watt
Junction capacitance at -6 V	1 pF
Breakdown voltage, V_B	60 volts
Cutoff frequency at V_B	150 Gc/s
Series loss resistance R_s	2.8 ohms
Average junction exponent	0.42

These specifications are characteristic of several RCA, Sylvania, and AEL varactors.

From (27), neglecting all losses except R_s ,

$$r(\text{at } 150 \text{ Mc/s}) = 34.7$$

$$r(\text{at } 750 \text{ Mc/s}) = 32.8$$

Since $R_1 = R_2 = R_s$ and $\alpha = 1$

$$\sqrt{\frac{\omega_1}{\omega_2}} = 0.187 \left(\begin{array}{c} \text{near curve } D \\ \text{Fig. 8} \end{array} \right) \quad \text{for } f_1 = 150 \text{ Mc/s}$$

$$\sqrt{\frac{\omega_1}{\omega_2}} = 0.42 \left(\begin{array}{c} \text{near curve } H \\ \text{Fig. 8} \end{array} \right) \quad \text{for } f_1 = 750 \text{ Mc/s}$$

we find, using Fig. 8, the pump-to-sideband conversion efficiencies,

$$\eta_{150} = \frac{4400}{4250} (0.75) = 77.5 \text{ per cent}$$

with m_1 max equal to 0.18

$$\eta_{750} = \frac{5000}{4250} (0.68) = 80 \text{ per cent}$$

with m_1 max equal to 0.15.

It must be emphasized that these calculated efficiencies are for a truly abrupt diode; exclude the effect of the parasitic package capacitance, circuit losses other than R_s , and coupling losses. The necessary impedance levels may be found by considering the results of the Appendix and Fig. 6, where,

$$\left[\frac{K_2}{R_2 R_3} \right]_{150 \text{ Mc/s}} = (0.18 r_{150})^2 = 39$$

$$\left[\frac{K_2}{R_2 R_3} \right]_{750 \text{ Mc/s}} = (0.15 r_{750})^2 = 24.2$$

Therefore, from Fig. 6, the normalized impedance R_N varies from 6.3 to 5.0 as the signal frequency is increased from 150 to 750 Mc/s. Considering the input to be a push-pull circuit, we find, using (25),

$$R_{g1} = R_{g2} = 8.8 \text{ to } 7.0 \text{ ohms}$$

$$R_L = 35.2 \text{ to } 28 \text{ ohms}$$

The calculated maximum pump power [(30) Fig. 9] is approximately 750 mW. An increase of this power to almost twice this value is permitted if we choose $\alpha = 2$, (22a). The new calculated conversion efficiencies are found to be approximately 73.0 per cent associated with a minor decrease of the values for $m_{1\text{max}}$ (Fig. 8; F, L).

An input filter was designed to match to an 16-ohm input impedance over the band of signal frequencies. The actual synthesis procedure will not be described here. This low-pass, coaxial structure was incorporated into the circuit shown in Fig. 13. The separation between the diode plane and the location of the input-output waveguide joining the diode-guide assembly was adjusted empirically for optimum power transfer. Since

this particular form of diode assembly places the diodes in a high-impedance section of guide, external tuning was necessary to adjust the effective impedance levels in both the pump and output circuits. The output load R_L was established in the diode plane using a slide screw tuner with a VSWR of 15 to 1. A similar device was used in the pump circuit, although only minimum tuning was required, since the probe structure coupling was optimized by the internal geometry and probe design.

C. Experimental Results

By tuning only the pump and output circuits, driving the signal input with an unmatched 50-ohm source, the following results were obtained with a pump power of 1.5 watts and a signal power of 200 mW.

Signal Frequency (Mc/s)	Conversion Efficiency
150	0.46
200	0.42
250	0.42
300	0.46
350	0.47
400	0.45

The allowable, theoretical pump power level is now found to be approximately 1.3 W. However, a drive power of 1.5 W was used without any appreciable deterioration in performance. Since the calculated power is based upon a limitation in allowable voltage swing, it is somewhat conservative, as some forward conduction is permitted to establish a regulating self bias. The fixed bias used was 25-volt (average) total, or 12.5 volts per diode. The theoretical bias would be approximately 32.5 volts, or 16.25 volts per diode for abrupt, fully-pumped junctions [see (35)].

VII. CONCLUSIONS

The abrupt-junction varactor diode enables the designer to convert microwave energy from one frequency to another with a high degree of efficiency and wide dynamic range. The actual effect of the device's non-linearity due to gain saturation upon information signals has not been considered in this paper. The intermodulation distortion has been shown to approach a limiting value of -17 dB as the output power approaches its maximum value [7].

The use of push-pull circuits provides sufficient isolation between the pump and output powers, permitting the exclusion of lossy, narrow-band filters in these circuits. Several wide-band, tunable converters have been built which demonstrate the reproducibility and efficiency obtainable from currently available varactors. Power outputs of greater than $\frac{1}{2}$ watt have been obtained at X band. Conversion efficiencies approaching 50 per cent at C band and 75 per cent at 500 Mc/s have been attained.

Although most of the currently available varactors have junction exponents which lie in the range $\frac{1}{3}$ to $\frac{1}{2}$,

the results achievable using varactors similar to those used in this design ($\gamma=0.42$) have demonstrated the validity of this design procedure. If varactors are used where $\gamma=\frac{1}{2}$ over the entire voltage swing, the efficiencies obtainable would approach those found in this analysis.

APPENDIX

ANALYSIS OF A THREE-FREQUENCY PUSH-PULL CIRCUIT

A simplified representation of a three-frequency, push-pull upconverter is shown in Fig. 14. The pump and signal currents i_1 and i_2 , respectively, drive the diodes in parallel with the polarities of the diodes reversed with respect to one another. The resulting sum frequency, idler current i_3 , circulates through both diodes in series and is dissipated in circuit losses and a load resistor R_L (not shown), which is effectively bypassed at the pump and signal frequencies. The idler current effectively cancels at the pump and signal port 1 due to the circuit balance (assuming identical diodes).

A fixed bias supply V_0 is connected so as to establish the necessary quiescent bias across the individual diodes. The required input and output matching networks will be determined.

Representing the charge on diodes *A* and *B* as

$$Q_a = \frac{Q_m}{2} + q_a \quad \text{referred to node 1} \quad (36)$$

$$Q_b = +\frac{Q_m}{2} + q_b \quad \text{referred to node 2} \quad (37)$$

where

$$q_a = (i_1' + i_2' - i_3)dt \quad (38)$$

$$q_b = (i_1' + i_2' + i_3)dt \quad (39)$$

$$i_1' = i_{1/2} \quad i_2' = i_{2/2} \quad (40)$$

the terminal voltages V_1 (at ω_1) and V_2 (at ω_2) at nodes 1) and 2) become

$$V_1(\omega_1) = 1/2 \left(R_s + \frac{S_m}{2j\omega_1} \right) i_1 + \frac{M_2 S_m}{\omega_3} i_3 \quad (41)$$

$$V_2(\omega_2) = 1/2 \left(R_s + \frac{S_m}{2j\omega_2} \right) i_2 + S_m Q_m M_1 M_3 \quad (42)$$

where (36)–(40) have been substituted in (4). The voltage at the output frequency ω_3 does not appear at this node. The effective output voltage appearing across R_L is the sum of the contributions from each diode where

$$V_3(\omega_3) = 2 \left(R_s + \frac{S_m}{2j\omega_3} \right) i_3 + \frac{M_2 S_m}{-\omega_1} i_1 \quad (43)$$

The necessary bias voltage V_0 becomes twice that

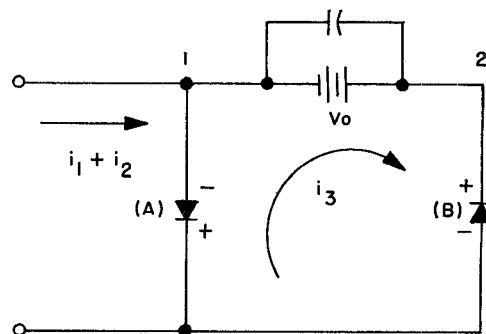


Fig. 14. Schematic representation of two varactors in push-pull circuit.

represented by (35). Assuming we tune the new elas-tance components in each circuit to resonance, the real input impedances may be evaluated from (41)–(43).

The pump and signal impedances, optimized for an impedance match become (using the criteria developed in Section IV and assuming the total loss to be R_s)

$$R_{g1} = R_{g2} \doteq \frac{1}{2} R_s \sqrt{X} \quad (44)$$

$$R_L \doteq 2 R_s \sqrt{X} \quad (45)$$

where

$$X \doteq 1 + \frac{m_1^2 \omega_c^2}{\omega_2 \omega_3} \quad (46)$$

The value of X has not been altered because of the push-pull mode of operation; therefore, the achievable efficiency represented in Fig. 7 remains the same (assuming identical diodes). The optimized impedance levels have changed, however, by a factor of two to one, as shown by (44) and (45). In addition, as expected, the allowable power input has been doubled.

ACKNOWLEDGMENT

The author is grateful for the technical assistance rendered by B. B. Bossard in the writing of the paper. In addition he would like to thank S. Perlman and E. Markard for their aid in the performance of the laboratory experiments which confirmed the operating characteristics of the devices discussed in the paper.

REFERENCES

- [1] Rafuse, R. P., and P. Penfield, *Varactor Applications*. Cambridge, Mass.: MIT Press, 1962.
- [2] Kotzebue, K. and L. Blackwell, *Semiconductor Diode Parametric Amplifiers*. Englewood Cliffs, N. J.: Prentice-Hall, 1961, pp 101–105.
- [3] Malchow, M. E., J. Curtis, L. Sickles, and J. Saultry, private communication.
- [4] Perlman, B. P., and B. P. Bossard, Efficient high level parametric upconverters, 1963 *IEEE Internat'l Conv. Rec.*, pt 3, pp 98–107.
- [5] Jackson, D., Large signal properties of nondegenerate varactor parametric amplifiers, presented at the 1962 IRE-Microwave Theory and Techniques Symp.
- [6] Markard, E., and S. Yuan, High-efficiency, high-order, idlerless frequency multipliers, using hyperabrupt varactors, *to be published*.
- [7] Interference reduction techniques for receivers, USAEL Contract DA-36-039-AMC-2345(E), U. S. Army Electronics Lab., RCA Adv. Microwave Tech., Group Comm. Sys. Div., New York, Jul 1963–Jun 1965.